Investigating the thermal performance of fibre reinforced polymer wall panel system in Waikato, New Zealand

Puviyarasan Velayudham , Krishanu Roy , Zhiyuan Fang , Chong Feng , Amirhosein Ghaffarianhoseini , James B.P Lim

PII: S0360-1323(25)00778-4
DOI: https://doi.org/10.1016/j.buildenv.2025.113298
Reference: BAE 113298

To appear in: *Building and Environment*

Received date: 17 April 2025
Revised date: 28 May 2025
Accepted date: 15 June 2025

Please cite this article as: Puviyarasan Velayudham , Krishanu Roy , Zhiyuan Fang , Chong Feng , Amirhosein Ghaffarianhoseini , James B.P Lim , Investigating the thermal performance of fibre reinforced polymer wall panel system in Waikato, New Zealand, *Building and Environment* (2025), doi: https://doi.org/10.1016/j.buildenv.2025.113298

Highlights:

- First empirical investigation of FRP wall panel system in residential building
- Indoor temperature remained within 18–24°C for 67.6% without mechanical cooling
- The 26 mm airgap mitigates heat transfer variability against outdoor fluctuations
- FRP as a climate-resilient alternative to conventional construction
- Material-specific thermal resistance and airflow dynamics for sustainable design

Investigating the thermal performance of fibre reinforced polymer wall panel system in Waikato, New Zealand

Puviyarasan Velayudham [a], Krishanu Roy [a*], Zhiyuan Fang [a], Chong Feng [a], Amirhosein Ghaffarianhoseini [c], and James B.P Lim [a, b]

E-mail: kris.roy@waikato.ac.nz

[a] School of Engineering, The University of Waikato, Hamilton, 3216, New Zealand

[b] Department of Civil and Environmental Engineering, The University of Auckland, Auckland, 1010, New Zealand

[c] School of future environment, Auckland University of Technology, Auckland, 1010, New Zealand

*Corresponding author: kris.roy@waikato.ac.nz

Abstract

The New Zealand building sector has long faced challenges such as inadequate insulation, indoor overheating and unhealthy living conditions, which are exacerbated by climate change, emphasising the need for innovative and climate-resilient material. In this study, the thermal performance of a novel fibre-reinforced polymer (FRP) wall panel system, including insulation in the cavity and an air gap, is experimentally examined in a case study building using field monitoring during peak summer conditions. Specifically, the impact of varying outdoor conditions and airflow on the indoor temperature, heat transfer through the walls, and air gap temperature were studied. The result showed that the indoor temperature of FRP panel system remained within the comfort range of 18-24°C for 67.6% of the observation period without mechanical cooling, outperforming conventional construction by about 10% in mitigating overheating. The air gap present in the system minimized temperature fluctuations by reducing heat transfer through wall and airflow (0.08 - 0.12 m/s) stabilised indoor temperature by reducing heat gain/loss variability. Furthermore, numerical simulation results aligned with experimental data within a 10% accuracy margin. This study provides the first

empirical evidence of FRP's viability as an alternative solution in New Zealand's climate, highlighting material-specific thermal resistance and airflow dynamics as critical design priorities for energy-efficient, climate-resilient housing to address escalating climate challenges.

Keywords: Fibre Reinforced Polymer (FRP) wall panel, Temperature, Thermal performance, Airflow, Heat transfer, Residential buildings

1 Introduction

Climate change and urban overheating together contribute to rising outdoor temperatures, with cities experiencing temperature increases of 4–10°C during heat events[1-4]. The rising temperatures impact building performance by accelerating material degradation, reducing thermal resistance and structural integrity [5] while increasing energy demands for heating and cooling compromising occupant comfort [2,3,6-9]. Research conducted by Ade et al. [10] investigated summer overheating in 29 houses in Auckland, New Zealand between January and March 2019 revealed that indoor temperatures remained within the comfort range (18–24°C) for only 35% to 57% of the time. This raises concerns about heat-related mortality and underscores the urgent need for resilient materials and innovative building envelopes to address thermal inefficiencies in a warming climate.

Other research works also reveal that the poor insulation in older homes increases energy demand, while mould and dampness caused by inadequate building envelopes frequently failed to maintain World Health Organization's (WHO) recommended indoor temperatures (18–24°C) [10-15]. In addition, global research highlights the material-specific thermal performance is highly dependent on local climatic conditions [6,7].

Rahiminejad et al. [16] demonstrated that wall composition dynamically influences thermal performance across varying conditions. Moreover, Roberz et al. [17] found that the ultra-lightweight concrete walls reduce heating demand by 7% compared to conventional structures, while lightweight steel-frame walls with superinsulation materials (SIM) achieve superior thermal efficiency despite their compact envelope thickness [18,19]. Studies on lightweight timber buildings suggest they perform well in moderate climates but struggle in hotter regions due to higher cooling demands [14,15,20]. This variation further emphasises the value of climate-adaptive construction through the development of steel-bamboo composite walls, which exhibited 32–45% higher thermal resistance than traditional timber walls in the winter [21]. Collectively, these studies highlight the critical role of region-specific, energy-efficient building envelopes (see Table 1).

Table 1 Summary of thermal performance and energy efficiency findings for various wall materials across different regions.

Ref	Region/year	Study focus	Method	Finding	Materials
[3]	New Zealand 2024	Impact of urban microclimate on energy consumption	Energy modelling	Urban morphology and characteristics influence local weather conditions.	Frame construction
[9]	New Zealand 2023	Thermal efficiency of construction materials	Systematic review	Composite materials show great potential for insulation	Different materials
[5]	Global 2021	Climate change impact on heritage typologies and materials	Systematic literature review	Climate change impacts cultural heritage buildings, leading to metal corrosion and material degradation.	Wooden buildings, concrete, and other construction materials
[22]	New Zealand 2020	Measuring the extent of thermal bridging in external timber-framed walls	Energy modelling	Built performance varies drastically due to the higher framing percentage, which increases thermal bridges.	Timber frame and timber studs

[19]	Israel 2019	Energy implications of FRP and concrete residential buildings	Numerical modelling	An FRP house has a higher cooling demand than a concrete house but performs better in the summer.	Concrete and Fibre reinforced polymer
[21]	China 2017	Thermal and energy performance of steel-bamboo composite walls	Experimental and field-testing	A steel-bamboo wall performs better than the other two wall types, reducing cooling and energy demand.	Steel-bamboo composite wall, Reinforced concrete wall and aerated concrete blocks
[15]	Europe 2017	Thermal response of lightweight timber building envelopes during cooling season	Dynamic thermal response analysis	The thermal behaviour and comfort of lightweight timber constructions can be improved through design and system modifications.	Light weight timber
[23]	New Zealand 2007	Potential and mechanical performance of FRP in NZ	Experimental testing	There is a need for an improved understanding of FRP in the New Zealand construction industry.	Fibre reinforced polymer

In New Zealand, 90% of residential buildings use timber framing, driven by material availability and historical market preferences [24]. However, conventional construction often creates persistent thermal performance issues, including thermal bridging, which undermines energy efficiency, increasing heating and cooling demands [9]. Research by Ryan et al. [22] found that timber frame construction uses over 34% timber, achieving thermal resistance (R-values) of 1.44 m²K/W, much lower than the previous estimate of R-values of 2.0 m²K/W. A study by Al-Rawi [25] on older homes in Waikato, New Zealand, identified an optimal indoor temperature of 22°C for thermal comfort and air quality. The Ministry of Business, Innovation and Employment (MBIE) in New Zealand further underscores the critical role of managing internal moisture as a key factor in maintaining healthy indoor environments [26,27]. Despite these issues, such as damp homes and condensation, are exacerbated by

ageing infrastructure, insufficient insulation, and poor design practices, leading to indoor discomfort, overheating, and increased hospitalisations [11,26,29,30].

In response, New Zealand revised its H1 energy efficiency building code, mandating stricter R-values for building envelopes (walls, roofs, floors, windows and doors) to advance net zero carbon target by 2050 [27,31]. Alongside these regulatory changes, the government actively promotes novel materials, innovative building systems, and advanced technologies to enhance construction resilience and efficiency[26,32]. Among these solutions, fibre-reinforced polymer (FRP) composites have gained widespread structural use internationally, while Marston's [23] research confirming their load-bearing potential in New Zealand.

Studies of FRP systems have indicated that they reduce air infiltration and heat loss in interfaces, achieving an R-values of 2.0 m^2K/W for a 75 mm thick panel with a foam core [33]. Additional studies emphasise FRP's thermal advantages such as minimised thermal bridging, and moisture resistance, making it ideal for damp-prone regions [23,33,34] . Furthermore, FRP materials demonstrate adaptable energy consumption patterns across seasonal and regional variations, proving suitable for fluctuating temperatures[19,33-35].

Marston's 2007 study [23] on FRP revealed its potential in structural application in New Zealand's building industry. In his research, he observed that to facilitate FRP's adoption and acceptance, further work is needed to provide the knowledge and understanding to prepare design codes and standards for its widespread use. To address this, FRP should be evaluated for its structural and thermal advantages, along with its long-term sustainable benefits.

Although FRP has been widely used in load-bearing applications globally, its use in New Zealand is limited to secondary applications such as cladding and architectural features [23]. It was not until 2024 that the first single-storey houses in Hamilton, Waikato, were completed

using FRP wall panel systems. Commercial testing confirmed that the wall panel system met New Zealand's standards for seismic resilience, air infiltration, and durability. For thermal performance, the system incorporated a phenolic rigid foam core and a 26 mm air gap, improving heat retention and airflow in walls (Figure 1). The system's mechanical and thermal properties, combined with flexible insulation configurations, improve performance in both moderate and extreme weather conditions.

While there is extensive research on the building thermal performance of conventional construction materials, a significant gap remains concerning FRP composites in New Zealand. No studies have specifically assessed the thermal performance of FRP wall panel system in this context, highlighting the need for real-time assessments of their regional suitability and impact on indoor comfort. This study evaluates the thermal performance of an FRP wall panel system, including insulation in the cavity and an air gap, using field monitoring during peak summer conditions (November 2023 to March 2024). It analyses outdoor conditions, airflow, indoor temperatures, and heat transfer dynamics. This study uses the experimental results and Integrated Environmental Solutions Virtual Environment (IES VE) simulation software to evaluate the FRP wall panel system's suitability for Climate zone 2 in New Zealand. The findings provide the first empirical evidence supporting its viability as a climate-resilient and energy-efficient alternative for residential construction in New Zealand.

(a) Lintel beams with phenolic foam rigid insulation

(b) Phenolic foam rigid insulation in corner

(c) Novel FRP wall panel system infilled with insulation

Figure 1 Novel fibre-reinforced polymer (FRP) wall panel system used in case study building.

2 Research approach

To evaluate the FRP wall panel system's viability in New Zealand's temperate climate, this study integrates experimental testing and numerical simulation to analyse temperature variations, heat transfer dynamics (loss/gain), and their impact on indoor thermal conditions (Figure 2). The study was conducted on a case study residential building located in Waikato, Climate Zone 2 (Figure 3), one of New Zealand's six climate zones—characterised by moderate winters (10–15°C) and humid summers (22–26°C) (22–26°C) [6]. The building was constructed under New Zealand's pre-2022 H1 energy efficiency code, enabling direct comparison with updated standards that mandate higher thermal resistance (R-values) or lower thermal transmittance (U-values) for walls [27,37] The methodology outlined in Figure 2 was followed to assess the thermal performance of the FRP wall panel system.

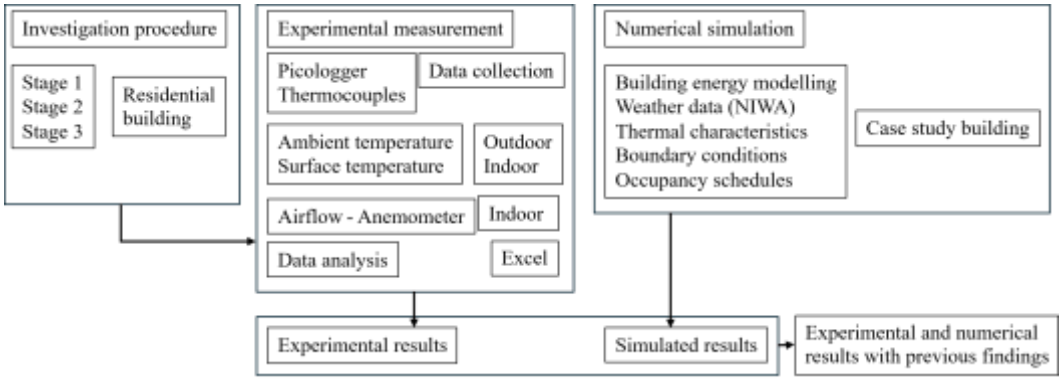

Figure 2 Flowchart of research methodology.

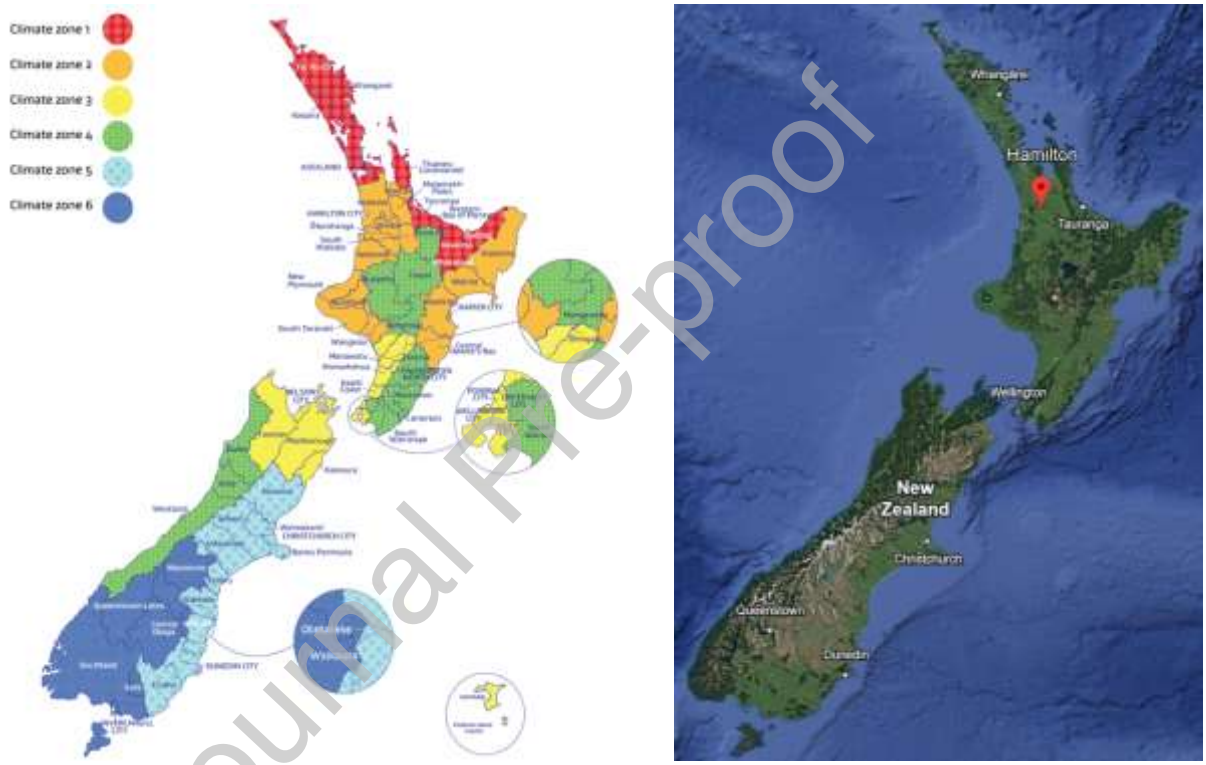

Figure 3 New Zealand's six different climate zones [6].

2.1 Experimental test set-up – Wall monitoring

Thermocouples paired with Pico loggers were used to monitor indoor and outdoor ambient and surface temperatures. A south-east oriented wall panel (1.4 × 2.2 m) was instrumented with 12 thermocouples, evenly spaced at 400 mm intervals, to capture internal and external surface temperature gradients. Two additional thermocouples measured indoor and outdoor air temperatures, positioned 20 cm away from surfaces to minimise radiative interference.

During stage 3, thermocouples were added to lintels, window peripheries, and partition walls to quantify localised heat transfer. An anemometer was positioned at the window opening and key airflow pathways to assess ventilation effects on indoor heat transfer and energy performance. All sensors recorded data at 1-minute intervals, with data aggregated into hourly and daily averages to balance high-resolution capture of transient events (e.g., rapid temperature changes) and seasonal trend analysis.

Data analysis adhered to ASHRAE 14 guideline [38] for measurement accuracy and reporting. Descriptive statistics of mean, minimum and maximum values were analysed to quantify the variability in temperature and airflow. These metrics were chosen to evaluate the thermal performance (peak overheating, diurnal fluctuations) and validate system resilience under extreme conditions. This methodology provided a robust framework for evaluating both transient and cumulative thermal behavior, aligning with best practices for building performance studies.

2.1.1 Temperature

Pico loggers with thermocouples are widely validated for thermal energy storage and heat flux studies[36,39-41], with ASTM/ISO standards recommending a minimum 72-hour monitoring period for reliable heat transfer assessment [42]. Vijayan et al. [43] highlighted the relationship between heat flow, temperature variations, and thermal resistance under varying indoor and outdoor conditions. This research utilises Pico loggers and thermocouples (Table 2) to measure temperatures and applies the thermal resistance of the novel FRP panel system to calculate heat flux. Thermocouples were calibrated using boiling water (99.6–100°C) and ice baths (0–0.3°C), achieving ±0.4°C accuracy in alignment with ISO 9869-1:2014 guideline for in-situ measurements [44].

Table 2 Specifications of the thermocouples, dataloggers and hotwire anemometer.

Sensor/data logger	Model	Number	Range	Accuracy
Thermocouple data logger	TC08 KJL56/178	8 channels	–270 up to +1820°C	-
	TC08 A0059/413	8 channels	–270 up to +1820°C	-
Thermocouple	Type K	16	–250 to +1370°C	±0.5ºC
Terminal board	Single channel	1	±70 mV	-
Humidity		1	5% to 95%	±5%
Hotwire anemometer	RSPro-8880	1	0.1 up to 25 m/s	±(5%+1d)

2.1.2 Airflow

Studies suggest that thermal comfort decreases by approximately 2°C when airflow velocities range from 0.07 m/s (winter) to 0.6 m/s (summer), a seasonal variation linked to occupants' adaptive behaviours and metabolic cooling [45]. Additionally, research recommends maintaining three air changes per hour (ACH) in summer and two ACH in winter to mitigate overheating and reduce energy consumption [46]. Long-term experiments in Fribourg, Switzerland, and shorter-term studies in Naples, Italy, have demonstrated links between outdoor temperature, airflow through cavities, and thermal resistance [16,36]. Khabaz A [47] found that varying air gap sizes significantly impact thermal transfer, with a 20 cm air gap reducing heat transfer by up to 93.5% compared to a conventional concrete wall. Full-scale experiments on walls have further shown that air gaps improve energy performance by enhancing heat recovery through cavity airflow[16,36,46-48] while increased airflow facilitates heat removal from the cavity.

In this study, airflow dynamics were assessed using a hot-wire anemometer (Table 2 and Figure 4e) positioned near window opening and 2m away from window when closed to measure velocities and temperatures during stage 3 monitoring. It evaluates how airflow influences heat influences heat removal and energy efficiency, building on the premise that increased airflow rates correlate with improved thermal resistance [16,45,46].

2.2 Investigation procedures

A unique approach to field investigation was carried out on a case study building at various construction stages to assess the impact of the FRP wall panel system on heat gain and loss. This research methodology consisted of three stages of recording indoor and outdoor temperatures in Building-1:

Stage 1: Building envelope with no internal walls and doors. This setup caused significant temperature variations and dynamic airflow (Figure 4e and f).

Stage 2: Interior doors were installed, and an insulated garage door was added (Figure 4g and h).

Stage 3: Semi-furnished house with no blinds. During weekdays, the house was occupied by a single resident (Figure 4i).

The research primarily focused on stage 3 due to its controlled occupancy and semi-furnished state, while data from stage 2 informed the analysis of cavity temperatures. Data collection was systematically documented across all stages, including sensor configurations, environmental conditions, and building modifications.

Figure 4a shows the placement of the sensors in the floor plan of building 1. The position of the thermocouples on the exterior surface of the south-east wall is illustrated in Figure 4b, while Figure 4c and 4d represent the cross-sections of I-I and II-II, providing detailed views of the external wall panel and internal partition wall panel systems. Thermocouples and an anemometer were placed in the kitchen to monitor indoor and outdoor heat transfers (Figure 4d). This configuration ensured comprehensive monitoring of thermal interactions between the building envelope and its environment.

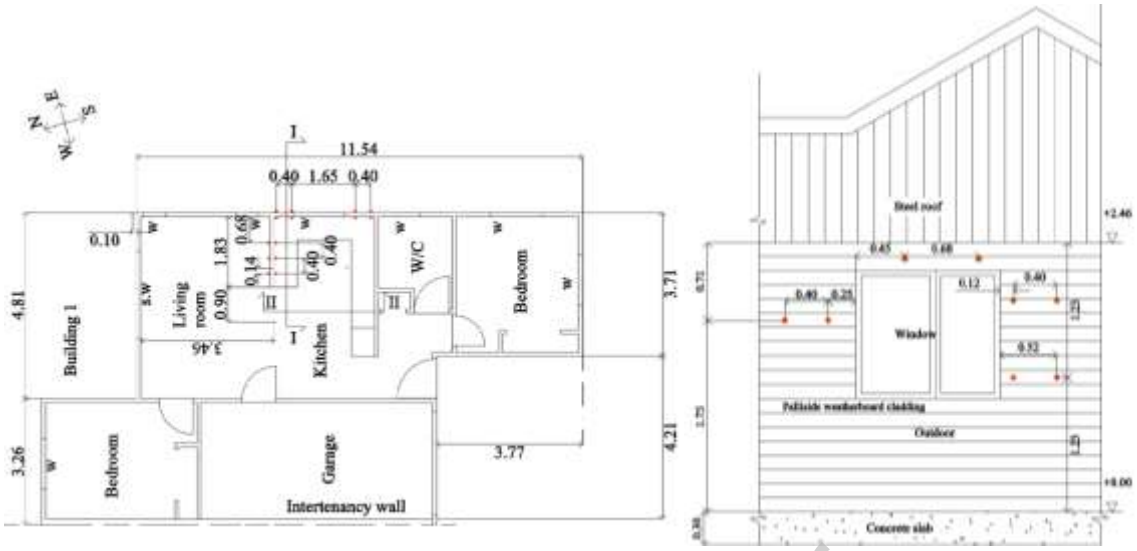

(a) Floor plan of the case study building (b) Side view of the case study building

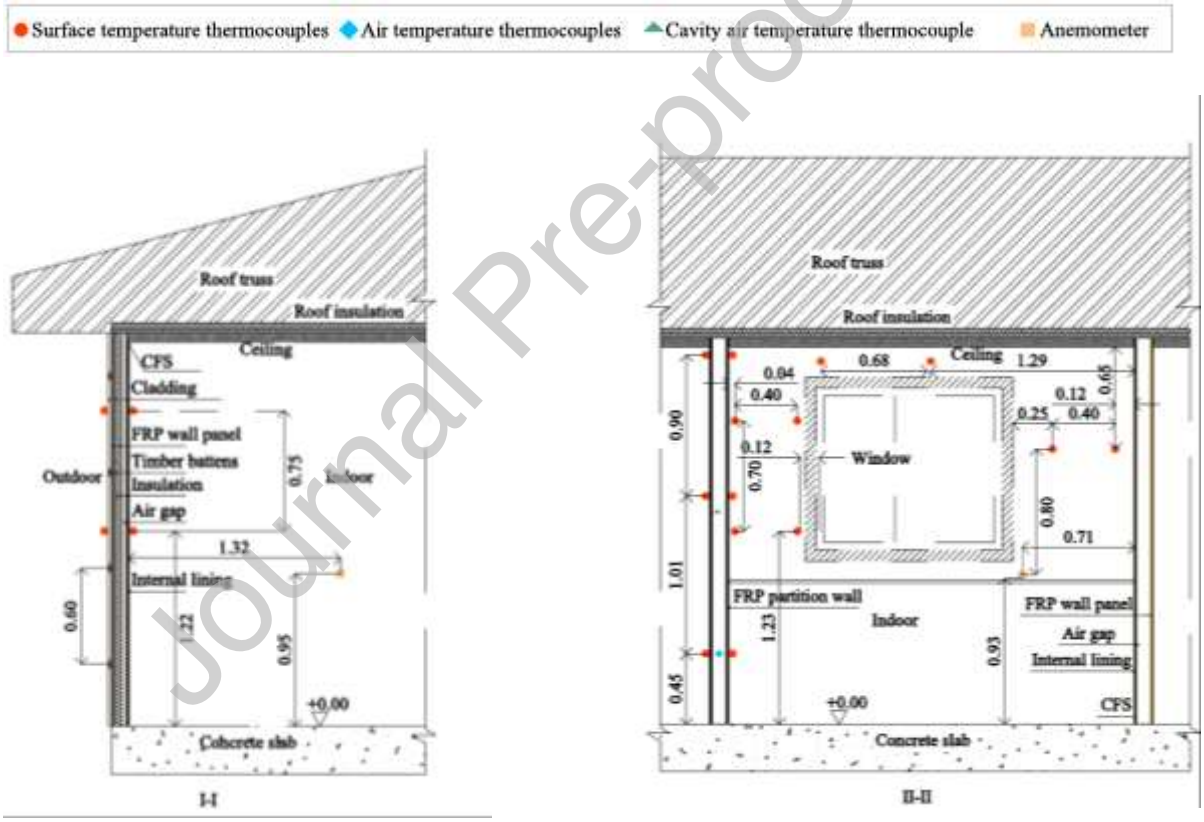

(c) Cross-Section I–I showing sensor positions in the case study building (All dimensions are in meters)

(d) Cross-Section II–II showing sensor positions in the case study building. (All dimensions are in meters)

Stage 1 – Case study building with no internal doors and temporary plywood inplace of garage doors, and thermocouple position for stage 1.

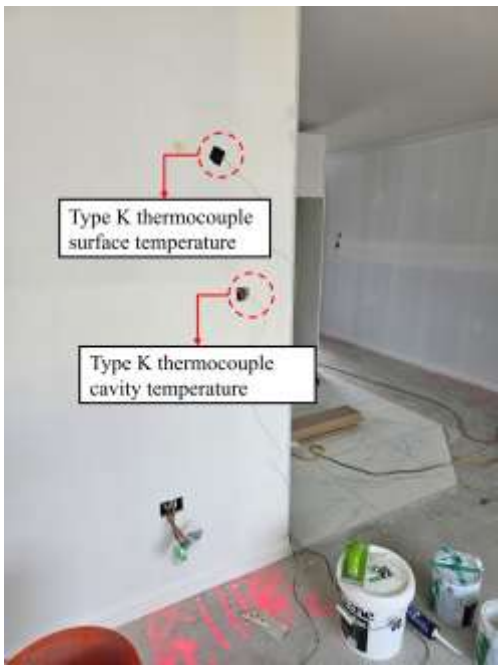

(e) Thermcouple positions on the partition wall

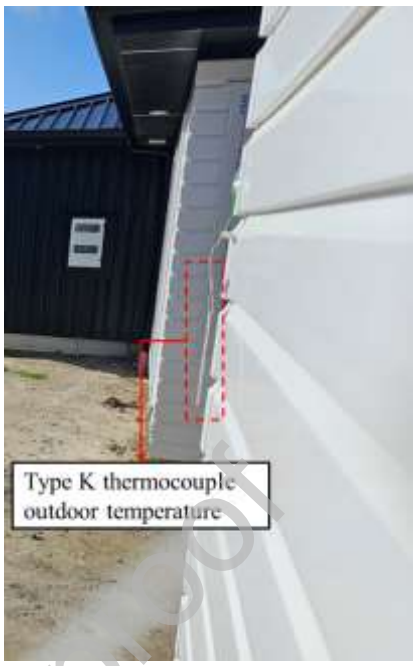

(f) Thermocouple position on the outdoor

Stage 2 – *Case study building with no internal doors but with insulated garage doors.

(g) Thermocouple positions on the indoor (top) and outdoor (bottom)

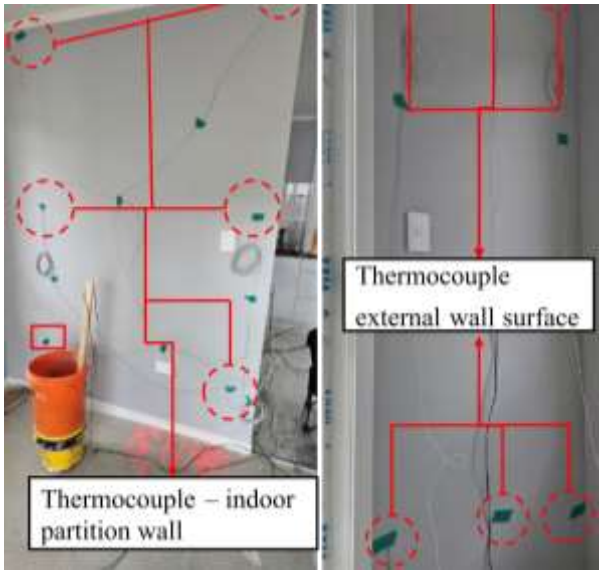

(h) Thermocouple positions on the partition walls (left) and external walls (right)

Stage 3 – **Case study building completed and thermocouple position.

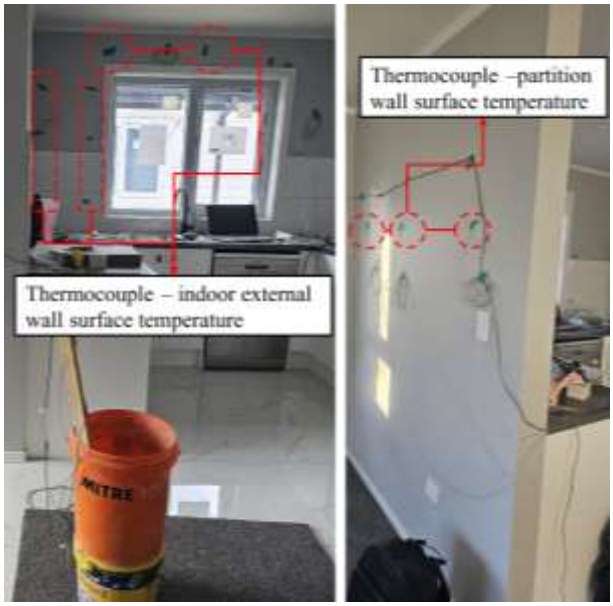

(i) Thermocouple positions on the surfaces of the external and partition walls (indoor)

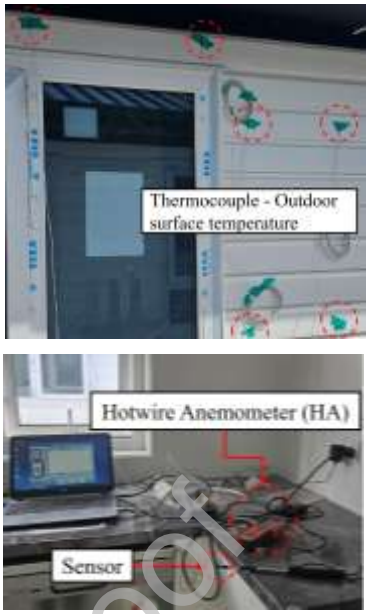

(j) Thermocouple positions on the surface of the external wall (outdoor)

* Internal doors were installed midway through the monitoring period to facilitate data collection ** The house was equipped with kitchen appliances and was occupied by one person on weekdays from 8 a.m. to 5 p.m. with partial occupancy. Notably, the house lacked internal shading as well as mechanical ventilation, heating or cooling systems during the data collection period.

Figure 4 Thermocouples and picologgers test set-up.

2.3 Description of the FRP wall panel system and a case study building

The FRP wall panel comprises thermoplastic resin, inorganic fillers, fire retardants, plasticisers, and organic fibres, formulated for non-combustibility (AS 1530.1), water resistance, and full recyclability. Each panel (0.45 m × 2.44 m) features three longitudinal cavities separated by vertical stiffeners, with 60 mm phenolic foam rigid insulation inserted into the cavities to create a 26 mm air gap (Figure 1 and 4c), a design optimised for thermal decoupling and moisture mitigation in external walls. The internal partition walls use the similar design but without insulation, forming an 86 mm air gap (Figure 4d). The FRP wall panel system assembly is capped with cold-formed steel (CFS) C-profiles at the top and

bottom. External walls feature rusticated white cladding, while internal walls are lined, resulting in a lightweight, non-homogeneous composite structure resistant to seismic and thermal stresses.

Figure 5a illustrates the floor plan of the case study building, which includes two bedrooms, a kitchen, a living room, a bathroom, and a garage. Figure 5b presents a 3D model of the case-study building, referred to as 'Building-1'. Building-1, the case study is a single-story duplex unit (gross floor area: 85.18 m²) representative of New Zealand's residential typology. It is constructed with a FRP wall panel system, steel roof, concrete slab foundation, and CFS framed intertenancy walls. The south-east oriented tested wall (3.2 × 2.44 m) features a window-to-wall ratio (WWR) of 0.27, selected to reflect typical New Zealand practices in temperate climate. The kitchen (15 m² monitored area) was prioritised for on-site investigations due to its accessibility and exposure to variable occupancy-driven thermal loads.

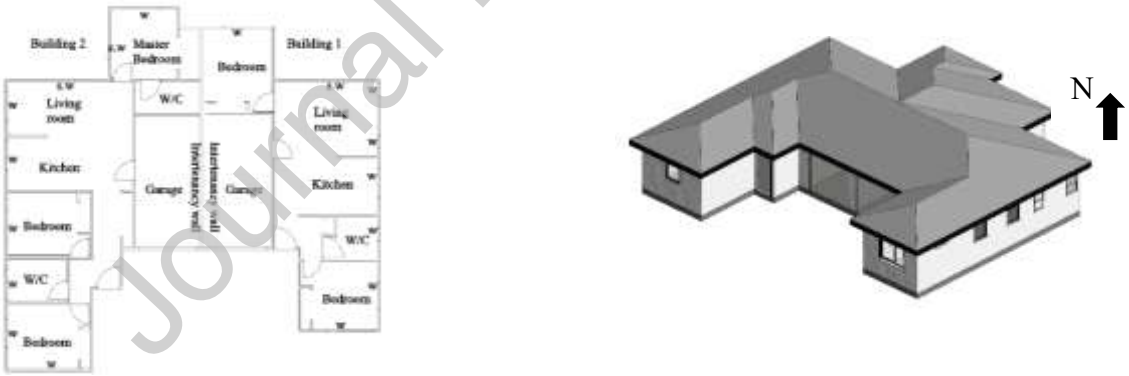

(a) (b)

Figure 5 (a) floor plan and (b) 3D model of the FRP case study building.

Thermal resistance values for all building elements are summarized in

Table 3. The FRP wall panel system incorporates an air gap design proven to mitigate thermal bridging by decoupling conductive pathways [47], along with interlocking joints that reduce air infiltration while enhancing thermal bridging resistance, as demonstrated by Abdou et al. [33]. This dual approach improves overall thermal efficiency by addressing both conductive (through insulation) and convective (via airtightness) heat transfer mechanisms.

The FRP panel itself exhibits a thermal conductivity (k) of 0.248 W/m·K, measured using a lambda thermal conductivity meter per ASTM C177. Using Equation 1, the system's total thermal resistance was calculated as 2.8 m²K/W, compliant with NZS 4214:2006 [37]. Air permeability testing further confirmed an average infiltration rate of 5.5 L/min/m², indicating low to medium air leakage performance consistent with industry benchmarks for energy-efficient envelopes. The role of the air layer in reducing thermal bridging has been well-documented in research conducted by Khabaz [47].

This study focuses on the overall thermal performance of the case study building constructed with the FRP wall panel system, without delving into detailed analyses of thermal bridging and air infiltration. The total thermal resistance of the building elements is calculated using the equation 1 provided in NZS 4214:2006 [49].

$$R_T = R_{si} + R_1 + R_2 + \cdots + R_{Se} \quad (1)$$

R_T = total thermal resistance, R_{si} = internal surface resistance, R_{se} = external surface resistance, $R_{1,2,3}$= thermal resistance of each layer

The heat transfer equation 2 used to calculate heat loss and gain [50].

$$Q = \frac{\Delta T}{R_T} \quad (2)$$

Where,

Q = Heat transfer through wall (W/m^2),

R_T = Total thermal resistance of the wall (m^{2}K/W),

ΔT = Temperature difference between internal and external surface (K).

And total heat loss (HL) equation 3 for the building proposed in NZBC – H1 [37]:

$$\mathrm{HL_{proposed}} = \frac{\mathrm{A_{roof}}}{\mathrm{R_{roof}}} + \frac{\mathrm{A_{wall}}}{\mathrm{R_{wall}}} + \frac{\mathrm{A_{floor}}}{\mathrm{R_{floor}}} + \frac{\mathrm{A_{glazing}}}{\mathrm{R_{window}}} + \frac{\mathrm{A_{door,opaque}}}{\mathrm{R_{door,opaque}}} + \frac{\mathrm{A_{skylight}}}{\mathrm{R_{skylight}}} \quad (3)$$

Table 3 Building envelope specifications.

Elements	Materials	R-Value m^{2}K/W
Perimetral wall	7mm FRP wall panel	2.8
	60mm phenolic foam rigid insulation	
	26mm airgap	
	7mm FRP wall panel	
	10mm Gib board	
Internal wall/ Garage partition walls	10mm Gib board	0.57
	7mm FRP wall panel	
	86mm airgap	
	7mm FRP wall panel	
	10mm Gib board	
Garage door	Insulated garage door	1.67
Window	4mm Low E +12mm argon + 4mm clear	0.63
Floor	300mm rib raft Pod Slab System	1.3
	20mm of carpet with padding	
Roof	30 mm corrugated metal roofing	4.83
	0.2 mm Flexible underlay	
	45 mm purlins	
	90mm insulations and rafter spacing.	
	25mm sofit board	

2.4 Building energy simulation parameters

The building energy simulation was performed using IES VE software [51], selected for its comprehensive whole-building simulation capabilities and compliance with ASHRAE standards [52]. The case study building was modelled with distinct thermal zones for each

room (Figure 6), with material properties detailed in Table 3. The building simulation parameters were defined in accordance with the New Zealand Building Code H1 acceptable solution/verification method [37] and ANSI/ASHRAE standards and guidelines [38,53]. Temperature constraints were set, with indoor temperatures maintained at 18°C for heating and 24°C for cooling. Occupancy was simulated for one person on weekdays from 8:00 a.m. to 5:00 p.m. with partial occupancy consistent with experimental setup, with no occupancy or appliance use on weekends. Internal gains were set at 150 W/person for occupant and plug loads were set at 24.5 W/m2 (equipment and lighting). Natural ventilation and infiltration settings were designed to reflect experimental conditions. Window and door openings were modelled in three intervals during weekdays (7:30a.m.–8:30 a.m., 12:30 p.m.–1:30 p.m., and 4:30 p.m.–5:30 p.m.) for 15 minutes each, while weekends remained closed to imitate real-time conditions. The infiltration rate was set to 5.5 L/min/m², derived from air permeability tests, and the airflow rate was set to 0.5 air changes per hour (ACH) as per the NZBC H1 code verification method [49].

The simulation utilised 1-minute timesteps, with results aggregated into hourly averages to align with the experimental data logging intervals. Due to constraints in data availability and the complexity of modeling, factors such as urban heat island (UHI) effects and the influence of adjacent buildings were excluded from the analysis. The study concentrated on critical thermal parameters, including occupancy schedules, temperature variations, and the thermal properties of materials, that directly impact heat transfer processes.

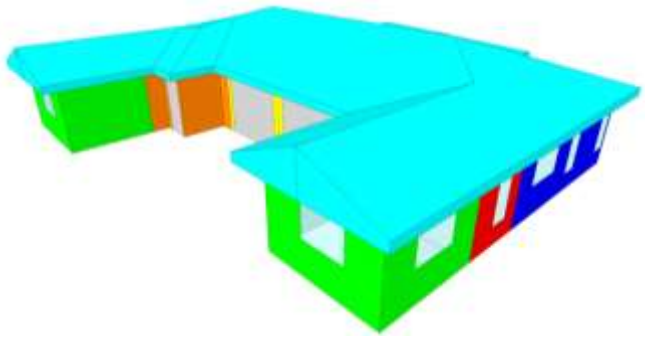

Figure 6 Distinct thermal zones of a simulated case study building.

2.4.1 Validation procedure

Various studies have indicated that validation outcomes are deemed acceptable when the margin of error falls within 10–20% [52,54,55]. Previous studies have typically used the coefficient of variation of the root-mean-square error (CV(RMSE)) and the normalized mean bias error (NMBE) to calibrate and validate models by comparing measured energy consumption with simulated or predicted values in whole-building simulations [17,54-58]. According to ASHRAE Guideline 14 [38], a model is deemed valid if the CV(RMSE) is within ±30% and NMBE is within ±10% for hourly data. The CV(RMSE) and NBME are defined in equations 4 and 5 below, where $\hat{y}_i$ is the simulated data,y_i is the measured data, $\bar{y}$ is the mean of the real data and n is the total number of data with p=1. Lower values of NMBE and CVRMSE indicates higher reliability and accuracy of the model.

$$CV(RMSE) = 100 \times \frac{\sqrt{\frac{\sum(y_{i=1}-\hat{y}_i)^2}{(n-p)}}}{\bar{y}} \quad (4)\ [54]$$

$$NMBE = 100 \times \sum_1^n \frac{(y_i-\hat{y}_i)}{((n-p)\times\bar{y})} \quad (5)\ [54]$$

In addition, previous studies have utilised indoor air temperature, outdoor air temperature, and surface temperature as key parameters for model calibration and validation [54,57,59]. In the current study, different construction stages of the FRP wall panel system (figure 4)

limited the direct comparison of energy consumption data. Therefore, hourly outdoor air temperature, indoor air and surface temperatures, were selected as calibration and validation parameters. These variables aligned with the simulation outputs, allowing direct comparison between measured and simulated data.

3 Results and discussions

The study focuses on temperature and airflow, prioritising quantification of the FRP wall panel system's ability to mitigate overheating under real-time summer conditions (Nov 2023–Mar 2024) directly exposed to outdoor environmental factors such as solar radiation, wind, and rain. Field monitoring during construction stages 1–3 introduced complexities including temporary occupancy shifts and exposure to variable outdoor conditions. Furthermore, temperature and airflow measurements were conducted to validate the findings, while accounting for instrument limitations. Thermocouples were positioned according to ISO 9869 [44] and hot-wire anemometer was added in stage 3 to assess airflow's role in indoor comfort. For the monitored wall, measurements averaged two to three thermocouples (±0.4°C accuracy), with data logged at one-minute intervals and aggregated into hourly/daily averages for seasonal trend analysis.

3.1 Temperature

The hourly and daily outdoor and indoor air temperatures from 00:00 on 19 January 2024 until 23:59 on 19 March 2024 were presented in Figure 7 (a) and (b). The data indicates that hourly outdoor and indoor temperatures reached up to 32.9°C and 29.9°C, respectively, while the daily outdoor and indoor temperatures were 26.9°C and 27.7°C, respectively. During the measurement period, indoor temperatures were maintained between 18°C and 24°C for 1,011 hours (67.6%) out of 1,494 hours and for 42 days out of 62 days, despite the absence of

mechanical ventilation (design limitations) and no active heating or cooling. The result indicated that the FRP wall panel system is within the comfort range, 10% higher than conventional construction (57%) in New Zealand [10].

The hourly and daily indoor and outdoor air temperatures are provided in Table 4. According to the data measured, maximum hourly indoor temperature of 29.9°C was recorded on 24 January 2024 peaking around 5:30 p.m., when outdoor temperatures ranged from 5.8°C to 32.9°C (range: 27.1°C) likely due to heat accumulation during the day in the absence of active ventilation. Conversely, the lowest indoor temperature was observed on 17 March 2024 ,when outdoor conditions overnight ranged from 5.8°C to 11.8°C (range: 6°C) between 8:30 p.m. and 8:30 a.m. Indoor air temperature stabilised at around 18°C but briefly dropped to 15°C around 7:30 a.m. on 18 March 2024, following occupant-induced door-opening. However, temperatures recovered to above 18°C shortly afterward, demonstrating the system's thermal buffering.

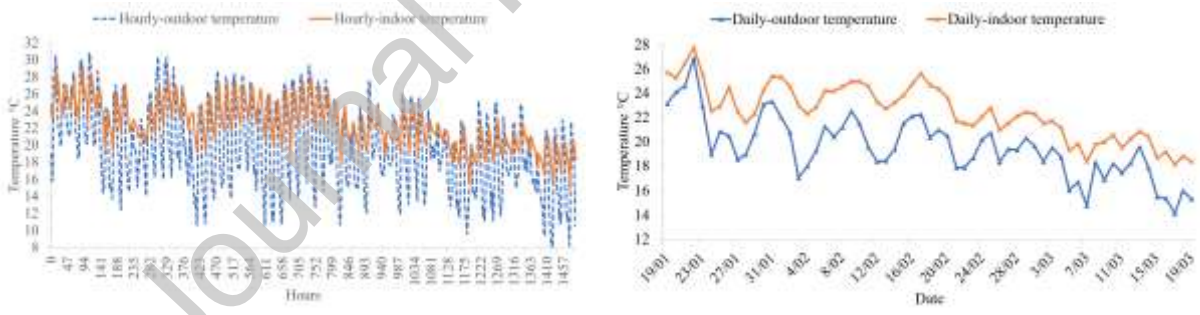

(a) (b)

Figure 7 Outdoor vs indoor air temperature from 19 January until 19 March 2024: (a) hourly and (b) daily.

Table 4 The hourly and daily temperatures of the FRP case study building

	Hourly temperature (°C)			Daily temperature (°C)			
Month	Min	Max	Mean	Min	Max	Mean	days

Indoor *	Nov-23	15.5	21.2	18.2	16.6	18.8	18.1	6
air temperature	Dec-23	16.3	20.9	18.9	18.5	19.7	18.9	6
	Jan-24	18.1	29.9	24.2	21.5	26.5	24.2	13
	Feb-24	17.7	28.1	23.6	20.8	25.8	23.5	29
	Mar-24	15.5	25.1	20.2	19.9	22.7	20.2	19
outdoor	Nov-23	9.4	30.1	15.9	12.9	18.5	15.5	6
air temperature	Dec-23	12.2	30.5	19	18	15.9	17.2	6
	Jan-24	11.9	32.9	21.8	17.8	25.7	21.7	13
	Feb-24	9.7	31.4	20.3	15.6	24.3	20.2	29
	Mar-24	5.8	28.2	17.5	10.4	21.2	17.3	19
Indoor	Nov-23	16.6	22.7	19.2	17.7	19.8	19.3	6
surface temperature	Dec-23	17	23.1	19.8	19.6	20.5	19.8	6
	Jan-24	20.8	30.3	25.2	21.9	27.8	25.3	13
	Mar-24	16.2	25.1	20.8	18.8	23.6	20.8	19
Outdoor	Jan-24	13	33.6	23.4	19.6	27.6	23.5	13
surface temperature	Feb-24	10.5	32.5	21.4	18.2	24	21.3	29
	Mar-24	6.6	28.3	17.8	10.5	20.6	17.5	19
Cavity air temperature	Nov-23	16.9	21.8	19.4	17.9	20	19.2	6
	Dec-23	17.2	22.4	19.9	19.6	20.6	19.9	6

* The lowest values were recorded in the morning when the occupant opened the door

The diurnal variations in cavity, outdoor, and indoor air and surface temperatures, in terms of hourly and daily behaviour, are shown in Figure 8 and 8b. These measurements were taken between 25 November 2023 and 6 December 2023 (stage 2) to analyse whether heat is stored in the cavity, and the temperature differences between the cavity and room air temperature. The hourly and daily cavity air temperature, indoor and outdoor air temperature are reported in Table 4. During this period, hourly indoor air temperatures ranged from 15.5°C to 21.2°C (range: 5.7°C), while daily temperatures fluctuated between 16.6°C and 19.7°C (range: 2.1°C). The hourly and daily cavity temperatures was consistently higher than the room temperature (see Figure 8). These surface temperatures were marginally lower than the cavity

temperatures but higher than indoor air temperatures, reflecting a system design in balance between cavity heat retention and indoor temperature.

The results indicate that the building system's air gap slowed heat transfer, improving indoor thermal comfort by storing heat in the cavity despite outdoor temperature fluctuations. Additionally, the indoor temperature increased as the outdoor temperature dropped, suggesting heat retention in the cavity. Hourly indoor temperatures remained between 15.6°C and 20.5°C (range: 5.1°C), while daily temperature ranged from 17.5°C and 19.4°C (range: 1.9°C). The cavity temperature was consistently higher than the room temperature (17°C to 22°C), as shown in Figure 8.

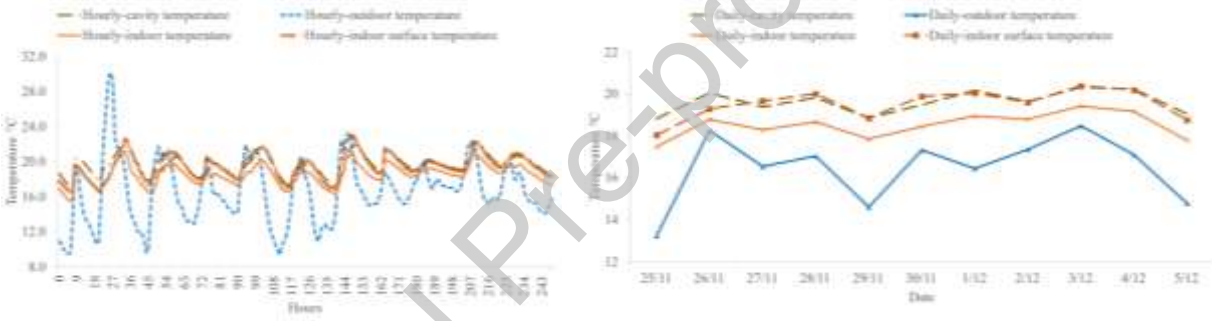

(a) (b)

Figure 8 Cavity vs outdoor, surface, and indoor temperature from 25 November until 6 December 2023: (a) hourly and (b) daily.

A consistent relationship between the room ambient temperature and indoor surface temperature were measured between 19 January 2024 to 19 March 2024 and illustrated in Figure 9, highlighting the FRP wall panel system's capacity to mitigate thermal fluctuations. Hourly indoor surface temperature had a range of 14.1°C while the external surface temperature had a range of 30°C, as shown in Table 4. Also, Figure 9a shows that the hourly indoor temperature variation closely follows the indoor surface temperature, while daily indoor air and surface temperatures followed similar trend as shown in Figure 9b.

Throughout the monitoring period, room temperatures remained within the range of both outdoor and indoor surface temperatures (Figure 9). As previously illustrated in Figure 8 the cavity temperature closely aligning with surface temperature less than room temperature demonstrating the heat retention in the cavity.

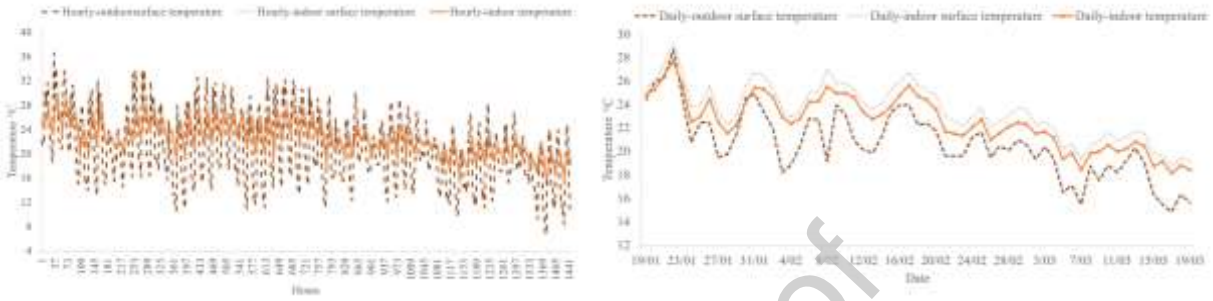

(a) (b)

Figure 9 Surface temperature vs room temperature from 19 January until 19 March 2024: (a) hourly and (b) daily.

Although this research was conducted between November 2023 and March 2024, heat loss and heat gain calculations focus on February 2024, which is New Zealand's peak summer month [60]. Previous studies have identified February as the hottest month in New Zealand's summer season [60], making it the most suitable period for evaluating the peak thermal performance. Hourly heat loss and gain were calculated using Equation 2 for February, with results illustrated in Figure 10. Indoor and outdoor surface temperatures are presented in Table 4. The recorded temperature ranges revealed distinct patterns across surfaces and indoor environments. The external surface exhibited the widest variation, fluctuating between 10.5°C and 32.5°C (range: 22°C), driven by outdoor air temperature swings from 9.7°C to 31.4°C (range: 21.7°C). In contrast, the internal surface and indoor air demonstrated smaller variations, the internal surface ranged from 19.7°C to 29.2°C (range: 9.5°C), while indoor air temperatures varied between 17.7°C and 28.1°C (range: 10.4°C).

During this period, the maximum heat gain was 3.86 W/m², while the maximum heat loss was 1.01 W/m², based on surface temperature variations through the measured wall. Figure 10 highlights the need for cooling when the indoor air temperature exceeds 24°C. Over 430 hours, indoor temperatures remained within the 18°C–24°C comfort range, compared to 106 hours at 24°C–25°C and 160 hours above 25°C. These deviations occurred under minimal natural ventilation (due to construction restrictions) and no mechanical ventilation (owing to design limitations). The results further indicate a total heat gain of 994.26 W/m² and a heat loss of 253.38 W/m² through the studied wall in February 2024. However, the indoor temperatures exceeded 24°C for 266 hours during this month, contributing to a heat gain of 425.86 W/m². This suggests that, while heat loss and gain occurred, the heat recovery potential of the FRP wall panel system mitigated these extremes thereby stabilizing indoor conditions despite outdoor variability.

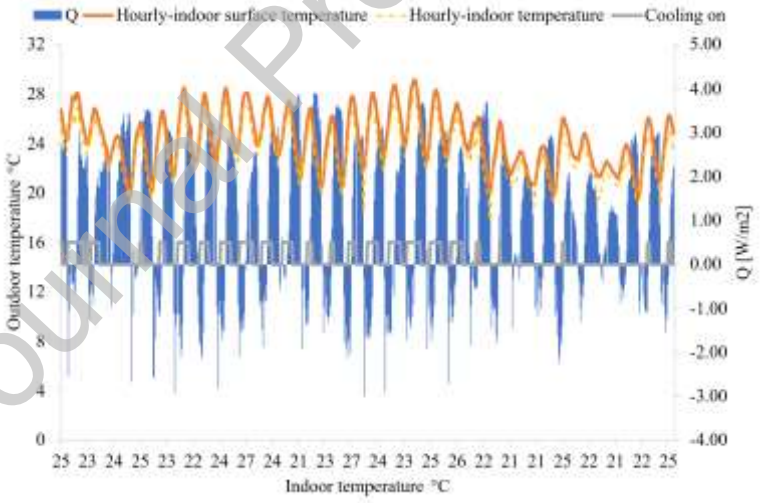

Figure 10 Heat loss and gain vs surface and indoor temperature of February 2024.

3.2 Air flow

Due to limitations in test kit availability, the airflow test was conducted between 16 April and 24 April 2024. Variations in indoor airflow, with windows both open and closed over a 75-

hour observation period, are illustrated in Figure 11. The analysis was conducted across three-time intervals, 5 p.m. to 11 p.m., 11 p.m. to 9 a.m., and 9 a.m. to 5 p.m. The results revealed that the airflow velocities ranging from 0.08 m/s to 0.12 m/s (mean: 0.11 m/s, range: 0.04 m/s) maintained indoor temperatures between 16.6°C and 19.6°C (mean: 18°C, range: 3°C), while outdoor temperatures varied significantly from 9°C to 29.3°C (mean: 17.5°C, range: 19.7°C). During the period from 9 a.m. to 4 p.m., airflow remained between 0.11 m/s and 0.12 m/s, sustaining indoor temperatures at 18.3°C despite outdoor fluctuations ranging from 16.3°C to 29.3°C (mean: 22.7°C, range: 13°C). From 11 p.m. to 9 a.m., airflow decreased to between 0.07 m/s and 0.12 m/s, with indoor temperature at 17.3°C and outdoor temperatures dropped to 12.4°C. This demonstrated consistent airflow regulation, ensuring indoor temperatures stayed above 18°C for most of the time without the reliance on ventilation.

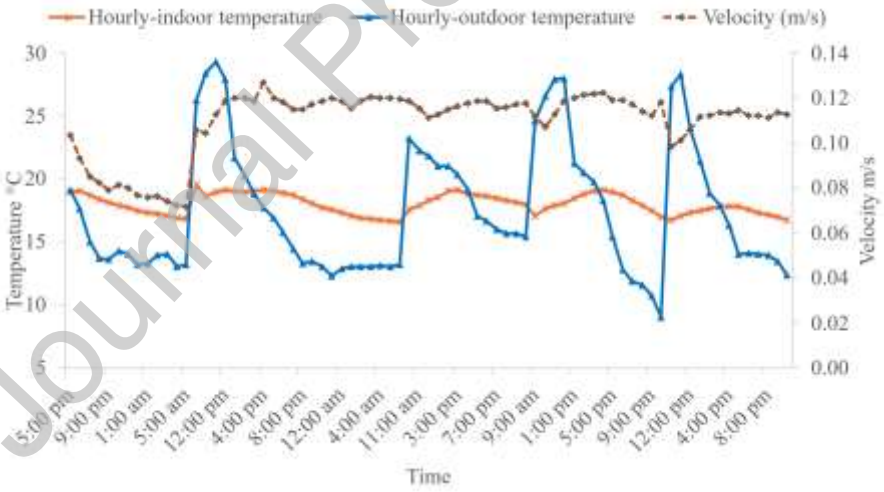

Figure 11 Airflow vs outdoor and indoor air temperature from 16 April until 24 April 2024.

3.3 Building energy simulation

3.3.1 Validation of the model

This study evaluated the thermal performance of a novel FRP wall panel system in a residential building, with results validated against experimental measurements according to ASHRAE 14 guideline [38,54]. Hourly comparisons of outdoor air temperature, indoor air temperature, and wall surface temperatures revealed the following discrepancies.

- Outdoor temperature: CV(RMSE) = 18.08%, NMBE = 7.18%
- Indoor temperature: CV(RMSE) = 8.72%, NMBE = -0.64%
- Indoor surface temperature: CV(RMSE) = 9.46%, NMBE = 3.72%

These values fall within the ASHRAE acceptable thresholds of ±30% (CV(RMSE)) and ±10% (NMBE) for hourly data [38], confirming the model's reliability. The relatively high CV(RMSE) for outdoor temperature (18.08%) likely reflects uncaptured urban heat island (UHI) effects and microclimatic variations in simulated weather data as observed in other studies lacking site-specific resolution [55,56].

The simulation employed weather data from NIWA's station, located approximately 10 km from the case study building [61]. In contrast, the experimental data captured localized conditions, including urban morphology and transient shading, resulting in monitored temperatures that exceeded simulated values by up to 3°C (experimental: 10.6°C to 30.5°C vs. simulated: 6.7°C to 29°C). This discrepancy aligns with findings by Converso et al. [59], who noted that weather station data often underestimates on-site temperatures in urbanized areas due to UHI effects. Similarly, a comparable study reported that in-situ urban temperatures surpassed weather file data by 2.2°C [56].

Further research in New Zealand has demonstrated that UHI-induced temperature increases can reach up to 4°C in dense residential areas, significantly impacting cooling demand and heat transfer dynamics [4]. For instance, a study analysing the impact of urban microclimate on residential building energy demand in Auckland found that the UHI effect led to an approximate 4.35% increase in cooling demand during summer and a 2.6% decrease in heating demand during winter [3].

The exclusion of dynamic variables, such as UHI effects, site-specific airflow patterns, transient shading, and adjacency effects, likely results in an underestimation of peak thermal stresses in the simulation. This limitation may affect the generalizability of the results to more complex real-world urban environments. To address these limitations, future work should incorporate localized urban boundary conditions and dynamic microclimatic modeling, including factors like shading dynamics, solar radiation, and wind velocity. Integrating such elements can enhance the predictive accuracy of energy-resilient designs and provide more reliable assessments of building performance in urban settings.

3.3.2 Simulation results

The simulation results were analysed to evaluate the thermal behaviour of the FRP wall panel system in February 2024, the peak summer month in Hamilton, New Zealand [60]. Hourly temperature fluctuations between experimental and numerical results are shown in Figure 12a. The weather data-derived outdoor temperatures ranged from 6.7°C to 29°C (mean: 18.3°C, range: 22.3°C), while field measurements recorded higher and more variable temperatures of 10.6°C to 30.4°C (mean: 20.3°C, range: 10.2°C). The wider range in field data likely reflects localized microclimatic effects (such as urban heat island influence, transient shading, or airflow variations) not fully captured by the model [57].

Simulated indoor temperature ranged from 21.3°C to 26.9°C (mean: 23.3°C, range: 5.3°C), while experimental indoor temperature varied from 17.7°C and 28.1°C (mean: 23.5°C, range: 10.4°C) exceeding the WHO recommended minimum temperature for thermal comfort [28,62]. The simulated indoor-outdoor temperature differences spanned from -4.3°C to 15.1°C, whereas experimental results showed a narrower range from -5.1°C to 10.3°C, indicating that the measured indoor temperature more closely followed outdoor fluctuations.

Despite discrepancies, both datasets revealed that the rising outdoor temperatures influenced indoor conditions without abrupt indoor shifts. The surface temperature in both the findings remained slightly higher than the indoor air temperature from 19.7°C to 29.2°C (measured) and 21.2°C to 26°C (simulated). These findings align with prior studies documenting increased cooling demand in Hamilton, New Zealand, driven by outdoor temperature impacts on indoor comfort [6].

Figure 12b compares daily temperature fluctuations. Simulated results demonstrated relatively stable indoor temperatures, despite outdoor variability, while measured data exhibited more pronounced diurnal variations. Daily simulated indoor temperature ranged from 22°C to 24.7°C (mean: 23.3°C, range: 2.7°C), compared to experimental values of 21°C and 25.6°C (mean: 23.4°C, range: 4.6°C). Simulated indoor-outdoor temperature differences spanned from 2°C to 7.6°C, whereas experimental results showed a narrower range of 2°C to 5.8°C. Notably, both methods indicated that indoor conditions followed outdoor temperature trends even in the absence of heating, cooling, or mechanical ventilation.

As shown in Figure 16, experimental outdoor temperatures exhibited greater variability than simulated data derived from NIWA [61]. The daily outdoor temperatures in the simulation ranged from 15.5°C to 22.2°C (mean: 18.3°C, range: 6.7°C), while measured values ranged

from 17.2°C to 22.5°C (mean: 20°C, range: 5.3°C). These differences are likely attributed to the absence of dynamic boundary conditions in the model such as transient solar gain, UHI effects, and occupant behaviour which are inherently present in real-world scenarios. This discrepancy may arise from differences between localized on-site environmental conditions (e.g., transient solar gain, vegetation effects, or occupant behaviour) and the static weather data input into the simulation. Although the simulation lacked certain localised parameters, it performed reasonably well in predicting indoor comfort: 71.2% of hours in the simulation fell within the thermal comfort zone, compared to 62.6% (8.6% lower) from the measured data, demonstrating the reasonable predictive utility of the IES VE software for assessments [52].

These results highlight the growing influence of warming climate on indoor environments, emphasizing the need for adaptive building designs to mitigate overheating risks. While IES VE simulations provide a strong framework for initial performance evaluations [51], discrepancies arise due to simplified boundary conditions. Incorporating site-specific microclimatic data (such as localized airflow patterns, transient shading, or material degradation) could improve the model's accuracy.

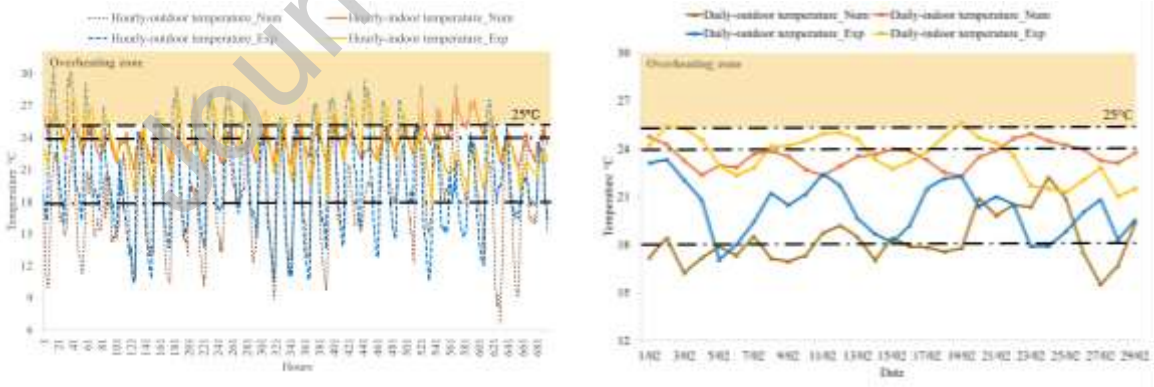

(a) (b)

Figure 12 Experimental versus numerical temperature of February 2024: (a) hourly and (b) daily.

3.4 Findings from this research highlighting the benefits of the FRP wall panel system

The experimental findings demonstrated that the superior thermal performance of the FRP wall panel system, compared to conventional framed construction, can be attributed to three interrelated mechanisms. Firstly, the air cavity present in the system acts as a dynamic thermal buffer, decoupling indoor conditions from outdoor extremes. During monitoring, cavity air temperatures remained stable within a narrow band of 17–22°C (Figure 8), providing approximately 5°C of thermal stability despite fluctuations in outdoor conditions.

Secondly, the FRP wall panel system combines low thermal mass materials with high thermal mass insulation, creating a hybrid structure that serves both as an air barrier and a thermal storage layer. This configuration balances rapid thermal responsiveness with delayed heat transfer, offering a performance advantage over conventional systems that typically rely on either high or low thermal mass alone. With a lower U-values of 0.357 W/m²·K (R-values of 2.8 m²·K/W), the FRP wall panel system significantly outperforms the 0.5 W/m²·K (R-values of 2 m²·K/W) benchmark required by conventional construction standards [37], while also fulfilling dual functional roles in thermal regulation.

Thirdly, the FRP wall panel system supports passive heat redistribution, which contributes to indoor thermal stability without reliance on mechanical heating or cooling systems. Heat accumulated in the cavity during warmer periods is gradually released during cooler night-time hours. These mechanisms collectively explain the 10% improvement in comfort duration over conventional construction despite the absence of mechanical ventilation.

The result suggests that current building code could evolve to recognise the benefits of integrated and dynamic thermal design strategies. For instance, New Zealand's H1 energy efficiency building code (acceptable solution) [37] could be extended to include performance

metrics such as thermal buffering capacity and thermal lag, rather than relying solely on steady-state R-values or U-values. Furthermore, the demonstrated benefits of the FRP wall panel system position it as a viable alternative solution for temperate climates particularly in affordable and social housing contexts, where energy performance directly affects occupant comfort and health.

This research focused on a case study building in Hamilton, New Zealand. The underlying design principles such as thermal decoupling, heat storage, and the use of hybrid materials that reduce dependence on mechanical systems are broadly applicable to similar climatic conditions, provided region-specific validation is conducted. Overall, this study highlights the potential of FRP wall panel systems as a climate-resilient and energy-efficient alternative, which is capable of mitigating overheating risks in a warming climate.

3.5 Comparison with previous studies

The thermal performance of building envelope materials varies significantly based on material type and thickness. For instance, hardwood timber walls with thicknesses of 0.140 m and 0.186 m achieved U-values of 0.152 W/m²·K (R-values of 6.58 m²·K/W) and 0.139 W/m²·K (R-values of 7.19 m²·K/W), respectively [16]. In contrast, steel–bamboo composite walls (0.17 m), reinforced concrete walls (0.28 m), and aerated concrete blocks (0.24 m) exhibited comparatively higher U-values of 0.6495 W/m²·K (R-values of 1.54 m²·K/W), 1.26 W/m²·K (R-values of 0.79 m²·K/W), and 0.88 W/m²·K (R-values of 1.14 m²·K/W), respectively, despite their greater thicknesses [17]. Similarly, aerated concrete walls with a thickness of 0.26 m recorded higher U-values of 1.799 W/m²·K (R-values of 0.56 m²·K/W), depending on material composition [47], while a lightweight steel-framed wall of 0.286 m thickness achieved a U-value of 0.314 W/m²·K (R-value of 3.19 m²·K/W) [18].

Research in New Zealand indicates that typical wall thicknesses range from 0.10 m in conventional construction to 0.19 m in green-certified homes [6,10]. The H1 energy code [37] mandates a minimum wall U-value of 0.50 W/m²·K (R-value of 2 m²·K/W), commonly associated with 0.10 m walls. Research by Ade et al. [10,11] on Auckland dwellings revealed that U-values range from 0.376 W/m²·K (R-value of 2.66 m²·K/W) in newer 6-Homestar homes to 0.741 W/m²·K (R-value of 1.35 m²·K/W) in older dwellings, with wall thicknesses between 0.10–0.19 m. Although concrete walls (0.19 m) in green-certified homes achieve lower U-values of 0.314 W/m²·K (R-value of 3.18 m²·K/W), they are associated with higher upfront costs and are prone to prolonged overheating [10,11]. In comparison, the novel FRP wall panel system (0.11 m) demonstrates lower U-values of 0.357 W/m²·K (R-value of 2.8 m²·K/W), outperforming conventional timber-framed wall systems, which typically reach R-values of up to 2.1 m²·K/W (0.14 m).

Previous research showed that the direct comparisons of overheating, heating and cooling demands remain complex due to dependence on local climatic conditions, material thermal properties, and construction timelines [6]. This study focuses on heating requirements when temperatures fall below 18°C and cooling needs when temperatures exceed 24°C. Research by Ade et al. [10], shows that various dwellings exceeded 24°C for 43–75% of hours between January and March 2019, while 70% of January to February hours in conventional buildings surpassed 25°C [11]. In contrast, the FRP case study building stayed above 25°C for only 19.75% above 25°C and 30.4% above 24°C.

Table 5 illustrates indoor temperature variations in relation to thermal resistance and outdoor temperatures. The case study building's indoor air temperatures ranged from 14.8°C on the coldest day to 29.9°C on the peak summer day (outdoor temperature 5.8°C – 32.9°C). Similar studies reported indoor air temperatures ranging from 7.8°C on a winter day in Aversa, Italy

[36] to 33.5°C on a peak summer day in Auckland, New Zealand (outdoor temperature 9.8°C - 29.1°C) [16]. Furthermore, higher R-values can improve thermal performance in some regions, they risk cold indoor temperatures or overheating in others, underscoring the need for region specific design.

Despite being in the same location (Auckland, New Zealand), two studies showed different room temperatures for walls with similar thermal resistance. This discrepancy underscores the importance of holistic design. Notably, the FRP wall panel system's integrated air cavity and airflow regulation help maintain a comfortable range most of the time, highlighting the importance of holistic design parameters like thermal storage and heat flux.

To evaluate the compliance of the case study building with the New Zealand Building Code (NZBC) H1 acceptable solutions [37], the total heat loss (HL) was calculated using Equation 3. The case study building's (built with pre 2022 building code requirement) overall heat loss was determined to be 274.21 kWh, which is 4% lower than the NZBC 2023 standards threshold of 285.54 kWh, even with restrictions on ventilation, heating, or cooling, demonstrating the effectiveness of this innovative system. Based on field investigations and building energy simulations, the novel FRP wall panel system used in the case study building demonstrated better indoor temperature control and comfort compared to most existing buildings in Glenns, Auckland [10], despite having similar climates to Hamilton.

Table 5 Summary of outdoor and indoor air temperatures with different R-Values.

			Outdoor temperature °C		Indoor temperature °C		R-value [m2K/W]
Ref	Location	Period	Minimum	Maximum	Minimum	Maximum	Wall
*	Hamilton, New Zealand	January-March	5.8	32.9	14.8	29.9	2.8

**	Hamilton, New Zealand	January-March	6.7	29	18.6	26.9	2.8
[3]	Auckland, New Zealand	Annual	8	24	19	29.5	2.04
[14]	Bridport, England	May-September	1	28.3	12.8	27.3	7.14
[10]	Auckland, New Zealand	January - March	9.8	29.1	19	33.5	2.10
[11]	Auckland, New Zealand	January - February	10.2	28.6	18.7	35.9	2.11
[36]	Aversa, Italy	December	4	21	7.8	20.5	2.78
[16]	Fribourg, Switzerland	Annual	0.8	21.5	18.3	25.5	7.19

* Case study-Temperature collected from the experimental results between 19 January 2024 – 19 March 2024

**Case study-Temperature collected from the numerical results between 19 January 2024 – 19 March 2024

Conventional timber and steel framing systems face persistent challenges, including thermal bridging, timber decay, and moisture accumulation influenced by multilayered building envelopes [9,30,63-65]. Overton's research on New Zealand wall assemblies demonstrated that most timber and steel frame assemblies fail to meet the ASHRAE 160 criteria for mould growth and corrosion when indoor relative humidity exceeds 70%, leading to condensation risks [30]. While timber-framed walls benefit from hygroscopic properties that mitigate condensation, they remain susceptible to decay when moisture content surpasses 20%. In contrast, steel-framed walls exhibit minimal moisture absorption but face higher condensation risks, with relative humidity reaching 100% at critical interfaces [30].

Comparative material testing of FRP panels under 500-hour condensation cycles revealed that the moisture uptake in timber is 88–91%, signalling significant decay risk, while uncoated

steel showed pronounced corrosion. However, FRP panels outperformed both materials, demonstrating minimal water absorption (0.37% mass gain) and no condensation risks. The 1000-hour neutral salt spray test showed no visible physical deterioration of the panel, while three point bending tests on field-aged samples (16 months) revealed only 5–9% mechanical degradation.

Critically, moisture accumulation in building envelopes is closely tied to orientation-dependent heat flux, which elevates condensation, fungal growth and mould risks in conventional constructions [66]. In conventional framed construction, condensation and dampness degrade wall insulation over time, impairing long-term thermal performance [67]. However, the design of the FRP wall panel system inherently mitigates these risks, as phenolic foam rigid insulation within the cavity is protected from high humidity and drastic heat flux fluctuations.

The phenolic foam core's moisture-resistant properties [68,69] combined with the panel system's low to medium air permeability (5.5 L/min/m²) and positive results in condensation testing, suggests a minimal risk of interfacial condensation at FRP joints. While FRP wall panel system is emerging as a promising alternative to conventional framing materials, further research is required to fully characterise the long-term hygroscopic behaviour of it in New Zealand's diverse climate zones.

3.5.1 End of life

FRP wall panel systems offer initial costs comparable to timber framing, with potential lifecycle savings attributed to minimal maintenance requirements, eliminating the need for treatments against rot or pests, and enhanced energy efficiency. Environmentally, FRP's recyclability, including the reuse of manufacturing waste into new panels, contrasts with

timber's biodegradability, which can be compromised by the use of toxic preservatives in New Zealand [65], and concrete's limitations in downcycling. However, the embodied carbon associated with FRP wall panels may be elevated due to reliance on imports from countries like China. This impact is partially mitigated by incorporating inorganic fillers such as fly ash into panel production [70]. To achieve carbon neutrality, localizing FRP manufacturing in New Zealand is critical, reducing transportation emissions and fostering local industry.

Adoption barriers for FRP in New Zealand include the absence of FRP-specific design codes, leading to reliance on standards like NZS 3604:2011 [71] , which are tailored for timber-framed buildings [31]. Additionally, unestablished supply chains pose challenges to widespread implementation. To advance FRP's role in climate-resilient construction, comprehensive lifecycle assessments (LCAs) are necessary to quantify net carbon savings accurately. Policy reforms should focus on integrating FRP-specific clauses into New Zealand's building codes and standards or establishing dedicated FRP composite standards. Such measures would ensure the viability and sustainability of FRP in climate-resilient design.

4 Conclusions and limitations

This study provides the first empirical evaluation of an FRP wall panel system in New Zealand’s climate zone 2, characterized by moderate winters and humid summers. The findings confirm the system’s potential to mitigate indoor overheating and improve thermal resilience. Additionally, the findings of this unique configuration of this system forming an air gap combined with insulation for temperate climate support New Zealand climate-resilient housing. While the findings highlight the viability of FRP systems in Waikato's temperate

climate (climate zone 2), conclusions regarding their suitability across New Zealand's diverse climate zones require further validation through field studies in representative regions.

Firstly, it was found that the indoor temperature of the FRP wall panel system remained within the comfort range of 18-24°C for 67.6% of the time of the observation period (outdoor max 32°C) without mechanical cooling. These results suggest the system could significantly reduce energy consumption compared to conventional residential buildings, where prior studies reported indoor temperatures exceeding the comfort range for 43–70% of the time. The FRP wall panel system's ability to maintain indoor comfort aligns with New Zealand's prioritisation of energy-efficient, healthy housing to combat overheating risks. Furthermore, the air gap in the system combined with low airflow rates (0.08–0.12 m/s) in rooms and through windows reduced heat transfer variability and stabilised indoor temperatures, minimising energy demands. Observed transient heat transfer through the wall system underscores the necessity of accounting for dynamic thermal behaviour in the building envelope design.

Secondly, validated numerical simulations using IES VE software (2024) aligned closely with experimental results, with CV(RMSE) and NMBE values for indoor air temperature at 8.72% and -0.64%, respectively within ASHRAE Guideline 14 thresholds. Surface temperature validation showed similar accuracy (CV(RMSE): 9.46%, NMBE: 3.72%), while the outdoor temperature CV(RMSE) was higher (18.08%) possibly due to limitations in the NIWA weather data. Nonetheless, the experimental and simulated results remained within acceptable thresholds, confirming the model's reliability in assessing overheating risk in Hamilton, Waikato (Climate Zone 2). These findings highlight that R-values alone are insufficient to evaluate thermal performance and emphasise the critical role of material-specific thermal behaviour and dynamic airflow design in climate-responsive building envelopes.

A case study building constructed with the FRP wall panel system exceeded 2023 H1 building code New Zealand by 4% emphasizing the need for region-specific accurate building modelling for cost-effective and energy-efficient designs. Results demonstrated that the system's air cavity functions as thermal resistance as well as heat storage, which aids in minimising heat loss and gain and enhancing thermal comfort, positioning it as a viable alternative to conventional materials in comparable climatic conditions.

The findings suggest a few practical recommendations: The New Zealand H1 energy efficiency building code (2023) should prioritise dynamic metrics such as thermal lag and thermal storage capacity when evaluating building envelopes, moving beyond traditional reliance on R-values. Additionally, FRP-specific design guidelines should be developed to address non-homogeneous material properties and incorporate regionally validated dynamic modeling, ensuring systems are tailored to local climatic conditions. Although this research focused on a specific case study in Hamilton, New Zealand, the underlying design principles such as thermal decoupling, heat storage, and the use of hybrid materials to reduce reliance on mechanical systems could be adapted to similar temperate climates, provided region-specific validation is undertaken. Such revisions would better reflect FRP's inherent thermal stability and resilience to overheating, reducing dependence on outdated assessment methods. Future codes should also integrate microclimatic variables and urban heat island effects that are currently overlooked, enabling more adaptive and climate-responsive building practices.

Despite promising results, this study has limitations. The FRP wall panel system's performance was evaluated exclusively in a single case study building in Waikato, focusing on temperature and airflow impacts. Other parameters, such as relative humidity and comfort indices, were excluded due to monitoring constraints during construction, occupancy, and post-occupancy stages. Although tests for condensation and accelerated corrosion confirmed

the durability of the panels, their long-term behavior in diverse environments requires further investigation to establish broader applicability.

Future research should explore the scalability of FRP wall panel systems in multi-storey designs and coastal/rural environments, integrating transient variables such as microclimate data and UHI effects into simulations. Addressing adoption barriers, including code compliance and supply chain limitations is essential. While this study addresses overheating risks in climate zone 2, targeted studies across New Zealand's varied climate zones are crucial to establish wider applicability. Furthermore, in-depth studies on economic viability and environmental impact should be conducted to ensure relevance in broader contexts. The findings provide a foundation for refining building codes and encourage further exploration of innovative materials in the pursuit of climate-resilient housing.

5 Acknowledgments

We would like to express our gratitude to Affordable Housing Solutions Limited and Mr Peter Jefferies, as well as to KZEL Holdings Limited and Ms Yang Zhou (Kelly) for providing the case study building and for their assistance with the house design. Additionally, we acknowledge the University of Waikato for providing the instruments and tools used in testing.

6 References

[1] M. Santamouris, "Recent progress on urban overheating and heat island research. Integrated assessment of the energy, environmental, vulnerability and health impact. Synergies with the global climate change," Jan. 15, 2020, *Elsevier Ltd*. doi: 10.1016/j.enbuild.2019.109482.

[2] Z. Jalali, A. Y. Shamseldin, and S. Mannakkara, "Evaluation of climate change effects on residential building cooling and heating demands in New Zealand: implications for energy efficiency standards and building codes," *International Journal of Building Pathology and Adaptation*, 2023, doi: 10.1108/IJBPA-10-2022-0168.

[3] Z. Jalali, A. Y. Shamseldin, and A. Ghaffarianhoseini, "Urban microclimate impacts on residential building energy demand in Auckland, New Zealand: A climate change perspective," *Urban Clim*, vol. 53, Jan. 2024, doi: 10.1016/j.uclim.2024.101808.

[4] Z. Jalali *et al.*, "What we know and do not know about New Zealand's urban microclimate: A critical review," *Energy Build*, vol. 274, Nov. 2022, doi: 10.1016/j.enbuild.2022.112430.

[5] E. Sesana, A. S. Gagnon, C. Ciantelli, J. A. Cassar, and J. J. Hughes, "Climate change impacts on cultural heritage: A literature review," Jul. 01, 2021, *John Wiley and Sons Inc*. doi: 10.1002/wcc.710.

[6] Z. Jalali, A. Y. Shamseldin, and A. Ghaffarianhoseini, "Impact assessment of climate change on energy performance and thermal load of residential buildings in New Zealand," *Build Environ*, vol. 243, Sep. 2023, doi: 10.1016/j.buildenv.2023.110627.

[7] Y. Kharbouch and M. Ameur, "Prediction of the impact of climate change on the thermal performance of walls and roof in Morocco," *International Review of Applied Sciences and Engineering*, vol. 13, no. 2, pp. 174–184, Aug. 2022, doi: 10.1556/1848.2021.00330.

[8] R. Yao *et al.*, "Evolution and performance analysis of adaptive thermal comfort models – A comprehensive literature review," Jun. 01, 2022, *Elsevier Ltd*. doi: 10.1016/j.buildenv.2022.109020.

[9] Y. Al-Radhi, K. Roy, H. Liang, K. Ghosh, G. C. Clifton, and J. B. P. Lim, "Thermal performance of different construction materials used in New Zealand dwellings comparatively to international practice – A systematic literature review," Aug. 01, 2023, *Elsevier Ltd*. doi: 10.1016/j.jobe.2023.106346.

[10] R. Ade and M. Rehm, "Summertime comparative evaluation of indoor temperature and comfort in Auckland New Zealand: a survey of green certified, code and older homes," *Building Research and Information*, vol. 49, no. 3, pp. 336–351, 2021, doi: 10.1080/09613218.2020.1712185.

[11] R. Ade and M. Rehm, "A summertime thermal analysis of New Zealand Homestar certified apartments for older people," *Building Research and Information*, vol. 50, no. 6, pp. 681–693, 2022, doi: 10.1080/09613218.2022.2038062.

[12] P. Howden-Chapman *et al.*, "He Kāinga Oranga: reflections on 25 years of measuring the improved health, wellbeing and sustainability of healthier housing," *J R Soc N Z*, vol. 54, no. 3, pp. 290–315, 2024, doi: 10.1080/03036758.2023.2170427.

[13] M. J. Nahlik, M. V. Chester, S. S. Pincetl, D. Eisenman, D. Sivaraman, and P. English, "Building Thermal Performance, Extreme Heat, and Climate Change," *Journal of*

Infrastructure Systems, vol. 23, no. 3, Sep. 2017, doi: 10.1061/(asce)is.1943-555x.0000349.

[14] T. O. Adekunle and M. Nikolopoulou, "Thermal comfort, summertime temperatures and overheating in prefabricated timber housing," *Build Environ*, vol. 103, pp. 21–35, Jul. 2016, doi: 10.1016/j.buildenv.2016.04.001.

[15] L. Pajek, B. Hudobivnik, R. Kunič, and M. Košir, "Improving thermal response of lightweight timber building envelopes during cooling season in three European locations," *J Clean Prod*, vol. 156, pp. 939–952, Jul. 2017, doi: 10.1016/j.jclepro.2017.04.098.

[16] M. Rahiminejad and D. Khovalyg, "Experimental study of the hydrodynamic and thermal performances of ventilated wall structures," *Build Environ*, vol. 233, Apr. 2023, doi: 10.1016/j.buildenv.2023.110114.

[17] F. Roberz, R. C. G. M. Loonen, P. Hoes, and J. L. M. Hensen, "Ultra-lightweight concrete: Energy and comfort performance evaluation in relation to buildings with low and high thermal mass," *Energy Build*, vol. 138, pp. 432–442, Mar. 2017, doi: 10.1016/j.enbuild.2016.12.049.

[18] L. Moga, I. Petran, P. Santos, and V. Ungureanu, "Thermo-Energy Performance of Lightweight Steel Framed Constructions: A Case Study," *Buildings*, vol. 12, no. 3, Mar. 2022, doi: 10.3390/buildings12030321.

[19] R. Reider and I. A. Meir, "Comparing the energy implications of FRP and concrete residential construction in a hot arid climate," *Energy Build*, vol. 186, pp. 98–107, Mar. 2019, doi: 10.1016/j.enbuild.2019.01.003.

[20] N. Maoduš, B. Agarski, T. Kočetov Mišulić, I. Budak, and M. Radeka, "Life cycle and energy performance assessment of three wall types in south-eastern Europe region," *Energy Build*, vol. 133, pp. 605–614, Dec. 2016, doi: 10.1016/j.enbuild.2016.10.014.

[21] Y. Li, J. Yao, R. Li, Z. Zhang, and J. Zhang, "Thermal and energy performance of a steel-bamboo composite wall structure," *Energy Build*, vol. 156, pp. 225–237, Dec. 2017, doi: 10.1016/j.enbuild.2017.09.083.

[22] V. Ryan, G. Penny, J. Cuming, I. Mayes, and G. Baker, "Measuring the Extent of Thermal Bridging in External Timber-Framed Walls in New Zealand," 2018.

[23] N. Marston, "Study report SR172 Fibre reinforced polymer composites," 2007.

[24] A. A. Dani, K. Roy, R. Masood, Z. Fang, and J. B. P. Lim, "A Comparative Study on the Life Cycle Assessment of New Zealand Residential Buildings," *Buildings*, vol. 12, no. 1, Jan. 2022, doi: 10.3390/buildings12010050.

[25] M. Al-Rawi, "The thermal comfort sweet-spot: A case study in a residential house in Waikato, New Zealand," *Case Studies in Thermal Engineering*, vol. 28, Dec. 2021, doi: 10.1016/j.csite.2021.101530.

[26] New Zealand legislation, "Building Act 2004 No 72 (as at 26 November 2024), Public Act 4 Principles to be applied in performing functions or duties, or exercising powers, under this Act – New Zealand Legislation."

[27] MBIE, "Transition of Building code 2021."

[28] N. Wimalasena *et al.*, "Environmental monitoring and thermal performance of New Zealand rental housing: an exploratory study," *Intelligent Buildings International*, vol. 14, no. 1, pp. 45–53, 2022, doi: 10.1080/17508975.2020.1845115.

[29] C. Beukes *et al.*, "Substandard South Auckland housing: findings from a healthy homes initiative temperature study," *Kotuitui*, vol. 19, no. 2, pp. 152–163, 2024, doi: 10.1080/1177083X.2023.2252038.

[30] G. Overton, "Study report SR344 Vapour control in New Zealand walls," 2016.

[31] A. Nwadike and S. Wilkinson, "Challenges facing building code compliance in New Zealand," *International Journal of Construction Management*, vol. 22, no. 13, pp. 2493–2503, 2022, doi: 10.1080/15623599.2020.1801336.

[32] I. & E. (MBIE) Ministry of Business, "Emerging trends in building design, technologies, and materials | Ministry of Business, Innovation & Employment," MBIE.

[33] O. A. Abdou ', K. Murali ', and A. Morsi ', "Thermal performance evaluation of a prefabricated fiber-reinforced plastic building envelope system," 1996.

[34] P. Cherian, S. Palaniappan, D. Menon, and M. P. Anumolu, "Comparative study of embodied energy of affordable houses made using GFRG and conventional building technologies in India," *Energy Build*, vol. 223, Sep. 2020, doi: 10.1016/j.enbuild.2020.110138.

[35] G. Tumminia, F. Guarino, S. Longo, M. Ferraro, M. Cellura, and V. Antonucci, "Life cycle energy performances and environmental impacts of a prefabricated building module," Sep. 01, 2018, *Elsevier Ltd*. doi: 10.1016/j.rser.2018.04.059.

[36] G. Ciampi, Y. Spanodimitriou, M. Scorpio, A. Rosato, and S. Sibilio, "Energy performances assessment of extruded and 3d printed polymers integrated into building envelopes for a south Italian case study," *Buildings*, vol. 11, no. 4, Apr. 2021, doi: 10.3390/buildings11040141.

[37] https://www.building.govt.nz/assets/Uploads/building-code-compliance/h1-energy-efficiency/asvm/h1-energy-efficiency-vm3-1st-edition.pdf, "H1 Energy efficiency building code," *MBIE*.

[38] "Measurement of Energy, Demand, and Water Savings." [Online]. Available: www.ashrae.org

[39] J. Sun, J. Xiao, Z. Li, and X. Feng, "Experimental study on the thermal performance of a 3D printed concrete prototype building," *Energy Build*, vol. 241, Jun. 2021, doi: 10.1016/j.enbuild.2021.110965.

[40] A. Shahcheraghian, R. Ahmadi, and A. Malekpour, "Utilising Latent Thermal Energy Storage in Building Envelopes to Minimise Thermal Loads and Enhance Comfort," *J Energy Storage*, vol. 33, Jan. 2021, doi: 10.1016/j.est.2020.102119.

[41] W. A. Qureshi, N. K. C. Nair, and M. M. Farid, "Impact of energy storage in buildings on electricity demand side management," *Energy Convers Manag*, vol. 52, no. 5, pp. 2110–2120, May 2011, doi: 10.1016/j.enconman.2010.12.008.

[42] N. Soares, C. Martins, M. Gonçalves, P. Santos, L. S. da Silva, and J. J. Costa, "Laboratory and in-situ non-destructive methods to evaluate the thermal transmittance and behavior of walls, windows, and construction elements with innovative materials: A review," Jan. 01, 2019, *Elsevier Ltd*. doi: 10.1016/j.enbuild.2018.10.021.

[43] D. S. Vijayan, A. Mohan, J. Revathy, D. Parthiban, and R. Varatharajan, "Evaluation of the impact of thermal performance on various building bricks and blocks: A review," Aug. 01, 2021, *Elsevier B.V.* doi: 10.1016/j.eti.2021.101577.

[44] ISO, “Thermal insulation — Building elements — In-situ measurement of thermal resistance and thermal transmittance Part 1: Heat flow meter method ,” *https://www.iso.org/standard/59697.html*, 2014.

[45] L. Yue and C. Zhongqing, “Seasonal thermal comfort and adaptive behaviours for the occupants of residential buildings: Shaoxing as a case study,” *Energy Build*, vol. 292, Aug. 2023, doi: 10.1016/j.enbuild.2023.113165.

[46] E. Conceição, J. Gomes, and H. Awbi, “Influence of the airflow in a solar passive building on the indoor air quality and thermal comfort levels,” *Atmosphere (Basel)*, vol. 10, no. 12, Dec. 2019, doi: 10.3390/ATMOS10120766.

[47] A. Khabaz, “Optimum thermal performance of green walls systems and design requirements against heat transfer of conventional external walls of low-rise concrete buildings in hot regions,” *Journal of Building Engineering*, vol. 78, Nov. 2023, doi: 10.1016/j.jobe.2023.107654.

[48] G. M. Girma and F. Tariku, “Experimental investigation of cavity air gap depth for enhanced thermal performance of ventilated rain-screen walls,” *Build Environ*, vol. 194, May 2021, doi: 10.1016/j.buildenv.2021.107710.

[49] Standards New Zealand, “Methods of determining the total thermal resistance of parts of buildings,” *NZS 4214:2006*, 2006.

[50] “Heat loss,” *Thermal Engineering, s.v. “What is Nusselt Number – Definition,” (accessed August 10, 2018), https://thermal-engineering.org/what-is-nusselt-number-definition/*.

[51] https://www.iesve.com/software/software-validation, “Integrated Environmental solutions limited”.

[52] A. I. , & R. S. N. Che-Ani, “Thermal environment accuracy investigation of integrated environmental solutions-virtual environment (IES-VE) software for double-story house simulation in Malaysia. ,” *Journal of Engineering and Applied Sciences*, vol. 14, no. 11, pp. 3659–3665, 2019.

[53] ASHRAE, “ASHRAE 55 - 2023,” https://www.ashrae.org/technical-resources/bookstore/standard-55-thermal-environmental-conditions-for-human-occupancy.

[54] G. Tomrukcu *et al.*, “A systematic approach to manual calibration and validation of building energy simulation,” *Smart and Sustainable Built Environment*, 2024, doi: 10.1108/SASBE-10-2023-0296.

[55] S. Shareef, “The impact of urban morphology and building’s height diversity on energy consumption at urban scale. The case study of Dubai,” *Build Environ*, vol. 194, May 2021, doi: 10.1016/j.buildenv.2021.107675.

[56] M. H. Elnabawi and N. Hamza, “A Methodology of Creating a Synthetic, Urban-Specific Weather Dataset Using a Microclimate Model for Building Energy Modelling,” *Buildings*, vol. 12, no. 9, Sep. 2022, doi: 10.3390/buildings12091407.

[57] G. Gennaro, E. Catto Lucchino, F. Goia, and F. Favoino, “Modelling double skin façades (DSFs) in whole-building energy simulation tools: Validation and inter-software comparison of naturally ventilated single-story DSFs,” *Build Environ*, vol. 231, Mar. 2023, doi: 10.1016/j.buildenv.2023.110002.

[58] B. Lin and Z. Chen, "Net zero energy building evaluation, validation and reflection – A successful project application," *Energy Build*, vol. 261, Apr. 2022, doi: 10.1016/j.enbuild.2022.111946.

[59] S. Converso, P. Civiero, S. Ciprigno, I. Veselinova, and S. Riffat, "Toward a Fast but Reliable Energy Performance Evaluation Method for Existing Residential Building Stock," *Energies (Basel)*, vol. 16, no. 9, May 2023, doi: 10.3390/en16093930.

[60] L. J. Harrington, "Rethinking extreme heat in a cool climate: A New Zealand case study," *Environmental Research Letters*, vol. 16, no. 3, Mar. 2021, doi: 10.1088/1748-9326/abbd61.

[61] I. and Employment. (n. d. -b). Ministry of Business, "Weather files for Aotearoa New Zealand. Building Performance," https://www.building.govt.nz/getting-started/climate-change-work-programme/resources/weather-files-aotearoa-new-zealand.

[62] N. N. Wimalasena, A. Chang-Richards, K. I. K. Wang, and K. N. Dirks, "What makes a healthy home? A study in Auckland, New Zealand," *Building Research and Information*, vol. 50, no. 7, pp. 738–754, 2022, doi: 10.1080/09613218.2022.2043138.

[63] A. Brambilla and E. Gasparri, "Hygrothermal behaviour of emerging timber-based envelope technologies in Australia: A preliminary investigation on condensation and mould growth risk," *J Clean Prod*, vol. 276, Dec. 2020, doi: 10.1016/j.jclepro.2020.124129.

[64] T. Singh, D. Page, and I. Simpson, "Manufactured structural timber building materials and their durability," *Constr Build Mater*, vol. 217, pp. 84–92, Aug. 2019, doi: 10.1016/j.conbuildmat.2019.05.036.

[65] G. Finch, G. Marriage, and N. Forbes, “Back to the future: The next 50 years,” 2017. [Online]. Available: https://www.researchgate.net/publication/321586450

[66] Y. Xue, Y. Fan, Z. Wang, W. Gao, Z. Sun, and J. Ge, “Facilitator of moisture accumulation in building envelopes and its influences on condensation and mould growth,” *Energy Build*, vol. 277, Dec. 2022, doi: 10.1016/j.enbuild.2022.112528.

[67] Samuel Hitch - buyinsulationonline, “Humidity and insulation damage,” N.d.

[68] F. Tariku, Y. Shang, and S. Molleti, “Thermal performance of flat roof insulation materials: A review of temperature, moisture and aging effects,” Oct. 01, 2023, *Elsevier Ltd*. doi: 10.1016/j.jobe.2023.107142.

[69] T. Ojanen, “Use of Rigid Phenolic Foam Exterior Insulation for Renovation of Concrete Sandwich Walls,” 2019. [Online]. Available: www.ashrae.org

[70] K. R. O’brien, J. Ménaché, and L. M. O’moore, “Impact of fly ash content and fly ash transportation distance on embodied greenhouse gas emissions and water consumption in concrete,” 2009.

[71] “NZS-3604:2011 - Timber-framed buildings,” *Standards New Zealand*, 2011.

Graphical abstract

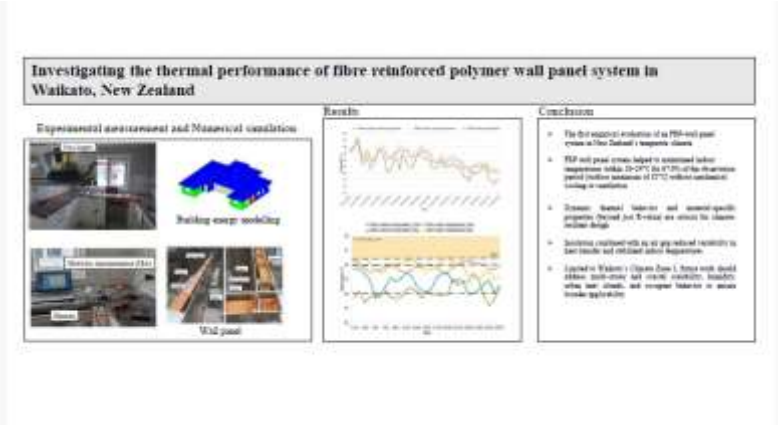

Declaration of interests

☒The authors declare that they have no known competing financial interests or personal relationships that could have appeared to influence the work reported in this paper.

☐The authors declare the following financial interests/personal relationships which may be considered as potential competing interests: